

Research Article

Antibacterial Effect of Dihydromyricetin on Specific Spoilage Organisms of Hybrid Grouper

Wenbo Huang ¹ and Jing Xie ^{1,2,3,4}

¹College of Food Science and Technology, Shanghai Ocean University, Shanghai 201306, China

²Shanghai Engineering Research Center of Aquatic Product Processing and Preservation, Shanghai 201306, China

³Collaborative Innovation Center of Seafood Deep Processing, Dalian Polytechnic University, Dalian 116034, China

⁴National Experimental Teaching Demonstration Center for Food Science and Engineering (Shanghai Ocean University), Shanghai 201306, China

Correspondence should be addressed to Wenbo Huang; wenbohuang1@163.com

Received 23 January 2021; Accepted 26 May 2021; Published 4 June 2021

Academic Editor: Laura Arru

Copyright © 2021 Wenbo Huang and Jing Xie. This is an open access article distributed under the Creative Commons Attribution License, which permits unrestricted use, distribution, and reproduction in any medium, provided the original work is properly cited.

This study aimed to investigate the mechanism of antibacterial activity level inhibition of dihydromyricetin (DMY) against specific spoilage bacteria of grouper. Firstly, the specific spoilage bacteria of grouper in the cold storage process are *Pseudomonas antarctica* (*P. antarctica*), which are selected by calculating the spoilage metabolite yield factor. It was determined that the minimum inhibitory concentration (MIC) and minimum bactericidal concentration (MBC) of DMY against grouper spoilage bacteria were 2.0 mg/mL and 6.4 mg/mL, respectively. DMY was added to the matrix of chitosan and sodium alginate, and DMY emulsions of different concentrations (0 MIC, 1 MIC, 2 MIC, 4 MIC) were prepared and characterized by differential calorimetry methods. Through analyzing cell permeability, enzyme activity, and images of the confocal laser scanning microscope (CLSM), we further studied the antibacterial mechanism of DMY emulsion on specific spoilage bacteria. The results showed that, with the increase of DMY concentration in the treatment group, the leakage of nucleic acid and protein increased significantly, the activity of ATPase and three critical enzymes in the Embden-Meyerhof-Parnas (EMP) pathway decreased significantly, and the activity of AKPase did not decrease significantly. The metabolic activity and viability are reduced considerably. Analysis of the above results shows that DMY inhibits the growth and reproduction of *P. antarctica* by interfering with the metabolic activity of bacteria and destroying the function of bacterial cell membranes but has no inhibitory effect on the activity of AKPase. This study proves that DMY could be an effective and natural antibacterial agent against specific spoilage bacteria in aquatic products.

1. Introduction

It is well known that aquatic products are very susceptible to spoilage caused by microorganisms. Therefore, it is necessary to develop effective antibacterial measures to maintain the freshness and quality of fish after slaughter [1]. Considering the hazards to health, chemical or synthetic additives are preferred to be substituted by natural preservatives. Recently, edible plant extracts have become increasingly popular ingredients in food processing research [2]. Polyphenolic compounds are the main components in plant extracts and are considered the most potent antioxidants in the human diet, and flavonoids account for the main

proportion of phenolic compounds. Moreover, flavonoids have been reported to have the potential of reducing the risk of many chronic diseases [3]. Therefore, they are combined into the nutritional and pharmaceutical products, and food to enhance products' health function [4].

Dihydromyricetin (DMY) is a flavonoid with high biological activity, and its content in vine tea can reach more than 30%, which is very rare and unique in the plant kingdom [5]. Some scholars have proved through in vitro experiments that DMY has anti-inflammatory effects [6, 7], antioxidant effects [8], and broad-spectrum antibacterial effects [9]. It can be seen that DMY has broad development prospects in the food industry as a bacteriostatic agent and

antioxidant. However, the antibacterial mechanism of DMY on spoilage bacteria has not been sufficiently studied.

Pseudomonas spp. is a common spoilage bacterium in aquatic products [10–12]. It is necessary to inhibit its growth and reproduction during storage and transportation for food safety. Although there are many antibacterial agents in applying fresh-keeping aquatic products, the research on DMY has not been involved. Therefore, this experiment studied the antibacterial activity of DMY against specific spoilage bacteria of grouper and developed DMY emulsion. Specifically, an emulsion was prepared to increase the availability of DMY during the preservation due to the low solubility of DMY. And to evaluate the efficiency of DMY emulsion, we measured the antimicrobial activity of dihydromyricetin (DMY) against specific spoilage bacteria of grouper and explored the mechanism of its antimicrobial function.

2. Materials and Methods

2.1. Activation and Inoculation of Strains. Through previous experiments [13], six strains were isolated. They screened from grouper under 4°C storage conditions, including *Shewanella putrefaciens* (*S. putrefaciens*), *Staphylococcus saprophyticus* (*S. saprophyticus*), *Pseudomonas azotoformans* (*P. azotoformans*), *Pseudomonas psychrophila* (*P. psychrophila*), *Pseudomonas antarctica* (*P. antarctica*), and *Pseudomonas koreensis* (*P. koreensis*). These strains were thawed at 4°C from –80°C and then added to 9 mL tryptic soy broth medium (TSB) liquid medium. In order to achieve an initial bacterial inoculum of about 10⁶ CFU/mL, they were shocked and stunned again after 1% transfer to make a bacterial suspension with OD of 0.3 and set aside.

2.2. Analysis of Spoilage Capacity of Spoilage Bacteria. Taking the spoilage metabolites (total volatile base nitrogen, TVB-N) produced at the end of the shelf life as an indicator, the research was conducted by calculating spoilage bacteria's spoilage ability. The spoilage metabolite yield factor $Y_{\text{TVB-N}/\text{CFU}}$ was calculated as shown in

$$Y_{\text{TVB-N}/\text{CFU}} = \frac{\text{TVB} - N_s - \text{TVB} - N_0}{\text{CFU}_s - \text{CFU}_0} \quad (1)$$

TVB–N₀ is the TVB–N content of grouper on day 0 after injection of the strain; the unit is mg N/100 g; TVB–N_s is the TVB–N content of grouper at the end of storage after the injection of the strain; the unit is mg N/100 g; CFU₀ is the total number of colonies in grouper on day 0 after inoculation, in log₁₀ CFU/g; CFU_s is the number of colonies in grouper at the end of storage after injection, in log₁₀ CFU/g.

2.3. Measurement of Minimum Inhibitory Concentration (MIC) and Minimum Bactericidal Concentration (MBC). The MIC and MBC analysis of the bacterial inhibitory capacity of DMY was performed using the broth microdilution method according to CLSI guidelines [14]. It was dissolved with 3% DMSO to obtain a 1.28 mg/ml DMY stock solution, and then serial two-fold dilution was performed in a 96-well

microtiter plate. The spare bacterial suspension was added and incubated at 30°C for 24 h. DMY's TSB medium served as a control group. Each 1 ml sample was diluted by decimal in a 0.85% (w/v) sodium chloride solution used for colony counting, and each concentration was repeated three times. The minimum concentration of DMY that inhibits the growth of visible bacteria was defined as MIC. The test group's bacterial suspension with no visible bacterial growth was also cultured on nutrient agar. The minimum concentration of DMY that resulted in no colony growth was defined as MBC [15].

2.4. Preparation of DMY Emulsion. According to the characteristics of dihydromyricetin, which is soluble in hot water but not in cold water, the dihydromyricetin emulsion was prepared by ultrasonic wave with chitosan, referring to the modified method of Woranuch and Yoksan [16] and Yang et al. [17], and the operation steps are shown in Figure 1. The dihydromyricetin with a concentration of 0 MIC, 2 MIC, 4 MIC, and 8 MIC was mixed with 2% Tween 80, and water was added. The mixture was homogenized at a speed of 15000 rpm using a homogenizer for 2 min and then sonicated to obtain a coarse emulsion. At room temperature, chitosan (Ch) (2%, w/v) was added to the acetic acid solution (1%, v/v) at 40°C and stirred for 4 h and filtered through a 1 μm pore filter, to remove the insoluble chitosan from the solution. Sodium alginate (SA) (1%, w/v) was added to CaCl₂ solution (0.1%, w/v), and Ch-SA was made by mixing 1.5 g glycerol, 170 ml Ch solution, and 300 ml SA solution mix the solution, then an equal volume of dihydromyricetin crude emulsion was added, and the mixture was homogenized with an ultrasonic homogenizer at 13000 rpm under ice bath conditions for 10 minutes to obtain 0 MIC, 1 MIC, 2 MIC, and 4 MIC dihydromyricetin emulsions.

2.5. Characterization of DMY Emulsion

2.5.1. pH. The pH of the emulsion was measured using a pH meter at room temperature. All measurements were repeated three times.

2.5.2. Differential Scanning Calorimetry (DSC). The method of Phunpee et al. [18] was adapted. The samples were weighed and placed in an aluminum pot with a lid and measured using nitrogen gas at a constant flow rate of 60 ml/min. A blank aluminum pot with a lid was used as a control and heated by a differential scanning calorimeter (Mettler Toledo DSC823e, USA) at a temperature range of 30 to 300°C by 10°C/min. The DSC was recorded for all sample curves. All measurements were repeated three times.

2.6. Microbial Cell Integrity. The cell membrane integrity can be assessed by detecting DNA, RNA, and protein leakage in the cell. After treatment with 0 MIC, 1 MIC, 2 MIC, and 4 MIC DMY at 30°C for 4 hours, the cells were collected by centrifugation (3000 r/min, 4°C, 10 min) and washed with 0.1 m PBS for three times, re-suspended in 0.1 m PBS

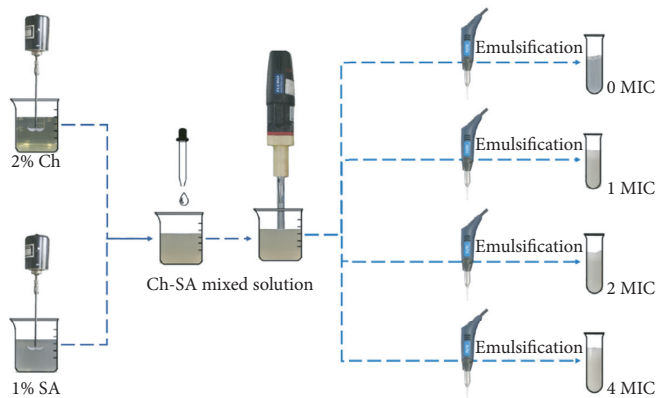


FIGURE 1: Flow chart of the preparation of Ch-SA stabilized DMYPickering emulsion.

solution, and immediately filtered the sample with 0.22 μm microporous filter. Absorbance readings were measured at 260 nm and 595 nm, and the number of nucleic acids and proteins released from the cytoplasm was determined by a UV spectrophotometer (UNICO UV-2100, USA) [19]. According to equations (2) and (3), the formula for nucleic acid is shown as follows:

$$\text{DNA concentration} = A_{260} \times 50 \mu\text{g/mL}, \quad (2)$$

$$\text{RNA concentration} = A_{260} \times 40 \mu\text{g/mL}, \quad (3)$$

where A_{260} is the absorbance value of the sample solution measured at 260 nm.

2.7. Using the Bicinchoninic Acid (BCA) Method to Measure Cell Permeability. The BCA protein determination kit got the protein leakage through the bacterial cell membrane. The OD value was measured at 562 nm using a UV spectrophotometer [20].

2.8. DMYPicks the Three Metabolic Pathways of EMP. The activities of hexokinase (HK), phosphofruktokinase (PFK), and pyruvate kinase (PK) in the EMP pathway of specific spoilage bacteria were tested with HK kit, PFK kit, and PK kit (Solarbio, Beijing Solarbio Science & Technology Co., Ltd.).

2.9. Cell Adenosine Triphosphate (ATPase) Activity Determination. ATPase assay kit (Jiangsu Jiancheng Institute of Biological Engineering) was used to test the inhibition of ATPase of specific spoilage bacteria by DMYPickering emulsion, and the absorbance value of the extract at 636 nm was obtained and analyzed using a UV spectrophotometer [15, 20].

2.10. Alkaline Phosphatase (AKPase) Activity. According to the manufacturer's instructions, the AKP activity was determined using the AKP kit (Nanjing Jiancheng Institute of Bioengineering, Nanjing, China). *P. antarctica* was cultured

in broth to a bacterial suspension with an OD of 0.3 and then mixed with DMYPickering nanoemulsions with concentrations of 0 MIC, 1 MIC, 2 MIC, and 4 MIC. The mixture was incubated in a shaking incubator at 30°C and 120 r/min for 4 hours. The sample was then centrifuged at 4°C, 3500 r/min for 10 minutes, and the supernatant was used to detect AKP activity [21].

2.11. Confocal Laser Scanning Microscope (CLSM). To evaluate the damage of bacterial cell membrane by DMYPickering treatment, CLSM (LEICA TCS SP5 II, Leica Microsystems, Germany) was used with dual fluorescence staining to analyze acridine orange/propidium iodide (AO/PI). AO emits green fluorescence and is used to stain live cells, while PI emits red fluorescence and is used to stain dead cells. The fluorescent dye was prepared by mixing 5 mg AO and 10 mg PI in 10 mL PBS (0.01 m, pH 7.2). In short, in the logarithmic growth phase, bacterial cells were treated with different concentrations of DMYPickering for 4 hours. Then, the bacteria with 100 μL of fluorescent dye in the dark were stained for 15 minutes while shaking gently. After washing with PBS and centrifugation, the cells were examined in an argon laser at 515/488 nm using CLSM. A control assay was performed without DMYPickering treatment [22].

2.12. Statistics and Analysis. All the results of physico-chemical determinations were presented as mean \pm standard deviation. Statistical analyses were performed using SPSS software (version 22.0; IBM Corp., Armonk, NY). One-way or multi-way analysis of variance (ANOVA) and Bonferroni statistical tests were used to determine the level of significance.

3. Results and Discussion

3.1. Analysis of the Spoilage Causing Ability of Spoilage Bacteria in Grouper. The spoilage potential of putrefying bacteria was expressed by the production of metabolites of spoilage bacteria per unit quantity (spoilage metabolite yield factor), as shown in Table 1. The total number of colonies of *P. psychrophila* and *S. putrefaciens* was 8.63 log₁₀ CFU/g and 8.23 log₁₀ CFU/g at the end of storage, respectively, which were significantly higher than those of the other four groups of spoilage bacteria. However, *P. antarctica* and *P. psychrophila* had the highest spoilage potential, while *P. koreensis* had the weakest. Moreover, the number of spoilage metabolites produced per unit number of *P. psychrophila* and *S. putrefaciens* was lower than *P. antarctica*. So, the metabolite production could be an indicator to reflect the spoilage potential of spoilage bacteria, and *P. antarctica* was selected as the target of the DMYPickering inhibition in this experiment.

3.2. MIC and MBC. Six dominant spoilage bacteria strains obtained from the screening of hybrid grouper were added to the DMYPickering dilutions. The TSB medium used as a control

TABLE 1: Analysis of the corrosion ability of grouper inoculated with specific spoilage bacteria at 4°C.

Strain name	Spoilage colony count log ₁₀ CFU/g		Decay product content mg N/100g		Spoilage metabolite yield factor $Y_{TVB-N/CFU}$
	CFU ₀	CFU _S	TVB-N ₀	TVB-N _S	
<i>Shewanella putrefaciens</i>	5.43	8.23	12.37	17.36	1.78
<i>Staphylococcus saprophyticus</i>	5.75	7.56	11.90	15.06	1.75
<i>Pseudomonas azotoformans</i>	5.71	7.28	11.56	14.37	1.79
<i>Pseudomonas psychrophila</i>	6.66	8.63	13.46	17.73	2.17
<i>Pseudomonas antarctica</i>	6.60	8.02	15.04	18.31	2.31
<i>Pseudomonas koreensis</i>	5.97	7.90	13.86	16.96	1.60

remained limpid, indicating that DMY was not contaminated. The results of MIC and MBC are shown in Table 2.

The results showed that DMY had a general inhibitory effect on all wild strains but a higher inhibition against *P. antarctica* with the MIC of 2.0 mg/mL and MBC of 6.4 mg/mL. The results indicated that DMY had a significant inhibitory effect on bacteria, which was consistent with the results of other researches [23, 24].

3.3. Characterization of DMY Emulsions

3.3.1. pH Variation of DMY Emulsions at Room Temperature Storage. As shown in Table 3, DMY emulsions had weak acidity, and with the increase of concentration, the pH value decreased. The pH values of 1 MIC and 2 MIC were observed to have a non-significant decrease throughout the storage, while the value of 4 MIC decreased significantly ($p < 0.05$).

3.3.2. Thermal Properties. DSC is an efficient thermal analysis technique that can characterize the samples' thermal properties and the formation of the embedding material [25, 26]. The DSC thermal spectra of CH, SA, CH-SA, 1 MIC DMY, 2 MIC DMY, and 4 MIC DMY are shown in Figure 2. In this experiment, except for DMY, which was in a dry powder state, all other samples were in solution or emulsion, so there was a downward exothermic trend initially, which may be related to the evaporation of water [27]. CH and SA had more profound heat absorption peaks at 162°C and 169°C, respectively. At the same time, the temperature range of the CH-SA thermal transition curve was 107–141°C, followed immediately by a small heat absorption peak. A heat absorption peak at 260°C can be found in the DSC thermal spectra of DMY, indicating its melting point. Comparison of the 1 MIC and 4 MIC emulsions of DMY mixed with CH-SA showed no heat absorption peak for dihydromyricetin, indicating that dihydromyricetin was encapsulated CH-SA.

In contrast, the emulsions of 1 MIC DMY, 2 MIC DMY, and 4 MIC DMY have independent endothermic peaks, and their melting points are significantly lower. The decrease in melting point indicates a reduction in sample stability and structural integrity [28]. However, the lack of independent endothermic peaks of DMY in the range of 263–285°C means that DMY and CH-SA have an interaction, confirming that DMY has been encapsulated or uniformly dispersed in the polymer mechanism in an amorphous state.

TABLE 2: MIC and MBC of DMY against specific putrefactive bacteria of hybrid grouper.

Strain name	MIC (mg/mL)	MBC (mg/mL)
<i>Shewanella putrefaciens</i>	3.2	>25.0
<i>Staphylococcus saprophyticus</i>	0.4	>25.0
<i>Pseudomonas azotoformans</i>	>25.0	>25.0
<i>Pseudomonas psychrophila</i>	3.2	8
<i>Pseudomonas antarctica</i>	2.0	6.4
<i>Pseudomonas koreensis</i>	6.4	16

Many scholars have found that the bound water in chitosan particles will reduce the endothermic peak [28–30]. Therefore, in this study, the endothermic peak changes of 1 MIC DMY, 2 MIC DMY, and 4 MIC DMY emulsions are due to the dispersion and interaction of DMY in chitosan particles.

3.4. Effect of DMY on Nucleic Acids and Proteins of *Pseudomonas antarctica*. The activities of bacteria are closely related to RNA, DNA, and proteins, so the integrity of cell membranes can be assessed by detecting the leakage of nucleic acids and proteins from the cells [19]. The leakage of nucleic acids and proteins from *P. antarctica* in 4 DMY treatments is shown in Figure 3. The amount of nucleic acid leakage in *P. antarctica* increased from 20.7 µg/mL to 78.3 µg/mL after 12 h of DMY treatment at 2 MIC concentrations. At the end of storage, the amount of protein leakage all increased to different degrees. It can be seen from Figure 3(b) that the protein leakage increased with increasing DMY concentration in the past. On day 12, the leakage of protein was only 48.2 µg/mL at 0 MIC concentration, while it was as high as 181.2 µg/mL in the 4 MIC group. And the protein leakage increased to 132.9 µg/mL and 152.8 µg/mL at 1 MIC and 2 MIC concentrations, respectively.

These results suggested that dihydromyricetin disrupted the cell membrane of *P. antarctica*, which led to leakage of proteins and nucleic acids. Di Pasqua et al. [31] explained the phenomenon that there were three hydroxyl groups in the chemical structure of DMY. The hydroxyl groups can bind to the cell membrane of bacteria through hydrogen bonding. And this interaction disrupted the cell membrane structure, which led to leakage of intracellular components. In these studies [9, 32], DMY showed its ability to significantly reduce membrane fluidity and act as an inhibitor of biofilm

TABLE 3: pH values at the beginning and end of 15 days of storage at room temperature for different DMY emulsions concentrations.

pH	Initial				15 days			
	0 MIC	1 MIC	2 MIC	4 MIC	0 MIC	1 MIC	2 MIC	4 MIC
	6.27 ± 0.67	5.42 ± 0.28	4.90 ± 0.11	3.16 ± 0.27	6.30 ± 0.17	5.29 ± 0.07	4.82 ± 0.09	2.73 ± 0.05

The symbol “±” indicates standard deviation.

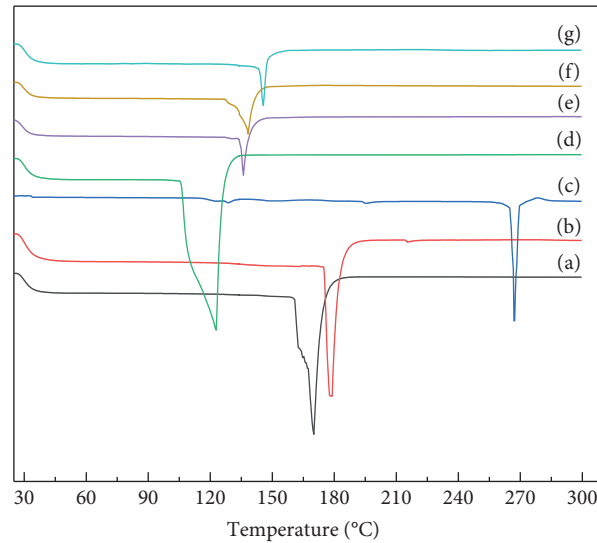


FIGURE 2: DSC analysis of the thermal properties of each component and the mixed emulsions. DSC thermograms of (a) Ch, (b) SA, (c) DMY, (d) Ch-SA, (e) 1 MIC DMY, (f) 1 MIC DMY, and (g) 1 MIC DMY.

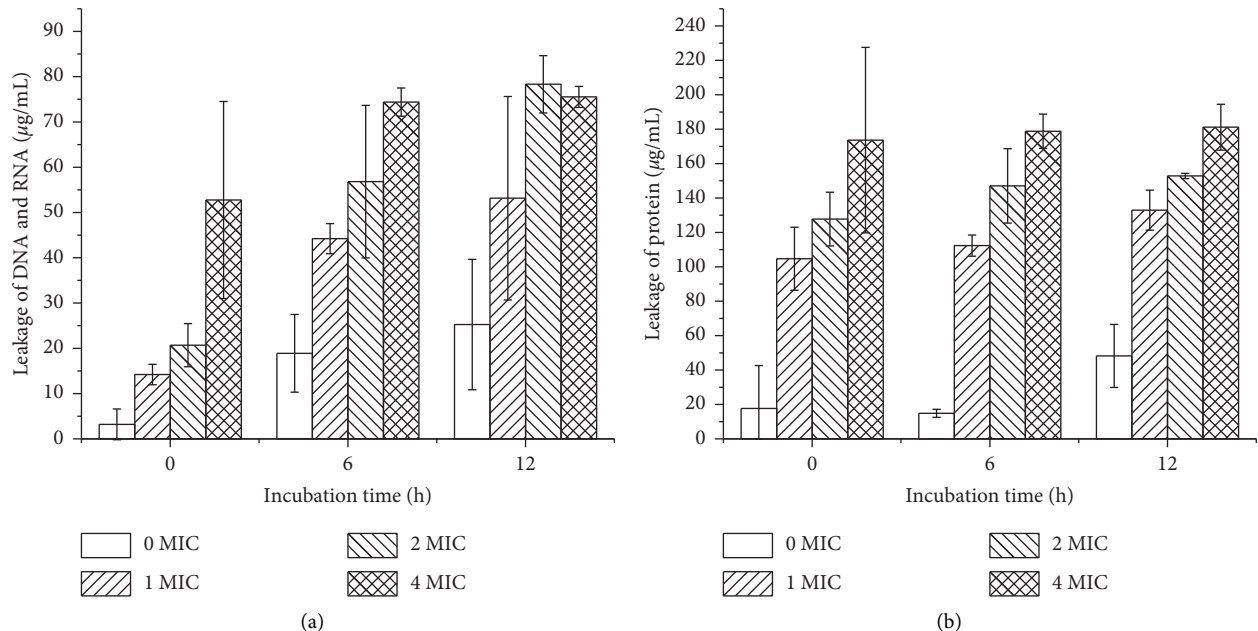


FIGURE 3: Leakage of DNA/RNA (a) and protein (b) from *P. antarctica* treated with DMY.

formation by interacting with phospholipids in the cell membrane. After breaking the first barrier, DMY caused leakage of intracellular nucleic acids and proteins by groove binding to intracellular DNA, further disrupting bacteria's normal function.

3.5. Effect of DMY on the Energy Metabolism of *Pseudomonas antarctica*. The energy metabolism of bacteria is closely related to the activity of ATPase [33, 34]. The results are shown in Figure 4. With different concentrations of DMY treatments, the ATPase activity decreased from 0.96 U/mg

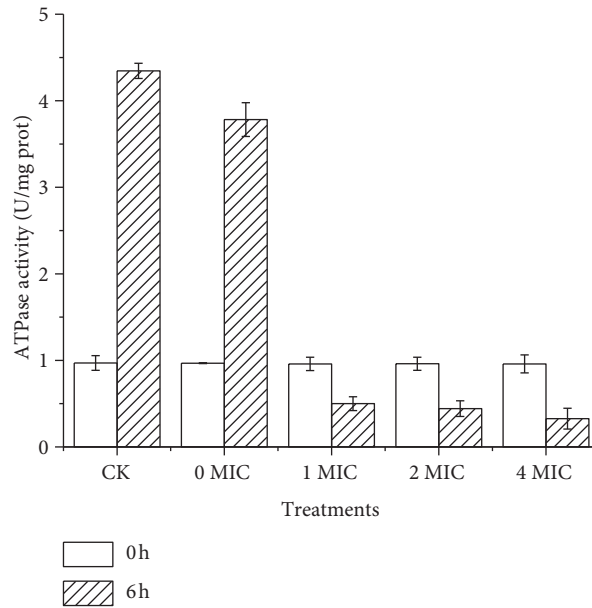


FIGURE 4: Effect of DMY on the ATPase activity of *Pseudomonas antarctica*.

prot to 0.50 U/mg prot, 0.44 U/mg prot, and 0.33 U/mg prot in the three treatment groups compared to the control group, with the most significant change in enzyme activity after DMY treatment at 4 MIC, decreasing by 65.6%. This result indicated that DMY had a significant inhibitory effect on energy metabolism in *P. antarctica* and demonstrated that DMY disrupted the bacterial cell membrane leading to ATP leak.

3.6. Effect of DMY on AKPase Activity of *Pseudomonas antarctica*. AKPase, which is present on the membrane between tissue cells and organelles, is a protease on biological membranes, and its action cannot be detected outside normal cells. Therefore, it can be used to measure the integrity of cell membranes [33]. As shown in Figure 5, there was no significant downward trend of AKPase activity in *P. antarctica* after DMY was treated in this experiment. It was indicating that there was no inhibitory effect on AKP activity despite the disruption of the bacterial cell membrane by DMY.

3.7. Effect of DMY on *Pseudomonas antarctica* EMP Pathway Enzymes. The glycolytic pathway (EMP) is an essential pathway for the production of ATP. It contains three irreversible reactions controlled by three vital regulatory enzymes (hexokinase, phosphofructokinase, and pyruvate kinase), so we can use the enzyme activities to study the mechanism of DMY inhibition on *Pseudomonas* spp. [33]. In the present study, DMY emulsions with 0 MIC, 1 MIC, 2 MIC, and 4 MIC concentrations were used to treat *P. antarctica* for 6 h. According to Figure 6, the three enzymes' contents were consistent among the groups at the initial point (0 h). As the time of DMY treatment increased,

the three enzymes' activities became lower in all three treatment groups than that of the control group, indicating that DMY can effectively inhibit *P. antarctica* by controlling the TCA pathway of respiratory oxidative metabolism.

3.8. Analysis of the Effect of DMY on the Metabolic Activity and Bacterial Viability of *P. antarctica*. A fluorescence microscope was used to verify whether DMY affected the growth and reproduction of *P. antarctica*. AO can penetrate the intact cell membrane and stain the nucleus of living cells with uniform green fluorescence; the nucleic acid in apoptotic cells can be spoiled with red fluorescence by binding to PI. Figure 7 shows the CLSM images at 1000x. In the control group without DMY treatment, the bacteria were almost all green, which indicated that the untreated bacteria were active. However, as the DMY concentration increased, the red fluorescence observed on the DMY-treated slides intensified, implying a gradual decrease in the number of live cells. The maximum red fluorescence intensity was observed in the DMY-treated group after 4 MIC. It was concluded from the image analysis that DMY inhibited the growth and reproduction of *P. antarctica*.

As shown in Figure 7, the results indicated that the metabolic activity of *P. antarctica* after treatment with DMY was significantly reduced. The metabolic activity of cells was reported to play a vital role in forming biofilms [35, 36]. Similar reports have been made for tea polyphenols and mangiferin acid [37, 38], and these antibacterial substances achieved inhibition by inhibiting biofilm formation. At the same time, a significant reduction in the metabolic activity of the cells was observed. Therefore, in combination with the CLSM image results, DMY inhibited the viability and metabolic activity of *P. antarctica* and significantly inhibited the formation of bacterial biofilms.

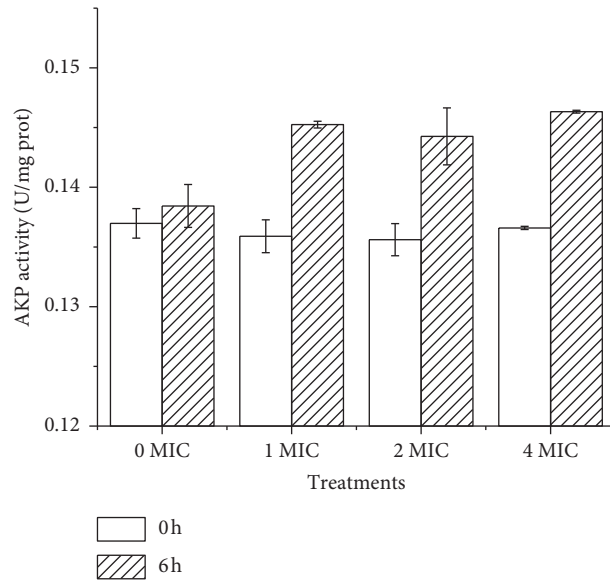


FIGURE 5: Effect of DMY on AKPase activity of *Pseudomonas antarctica*.

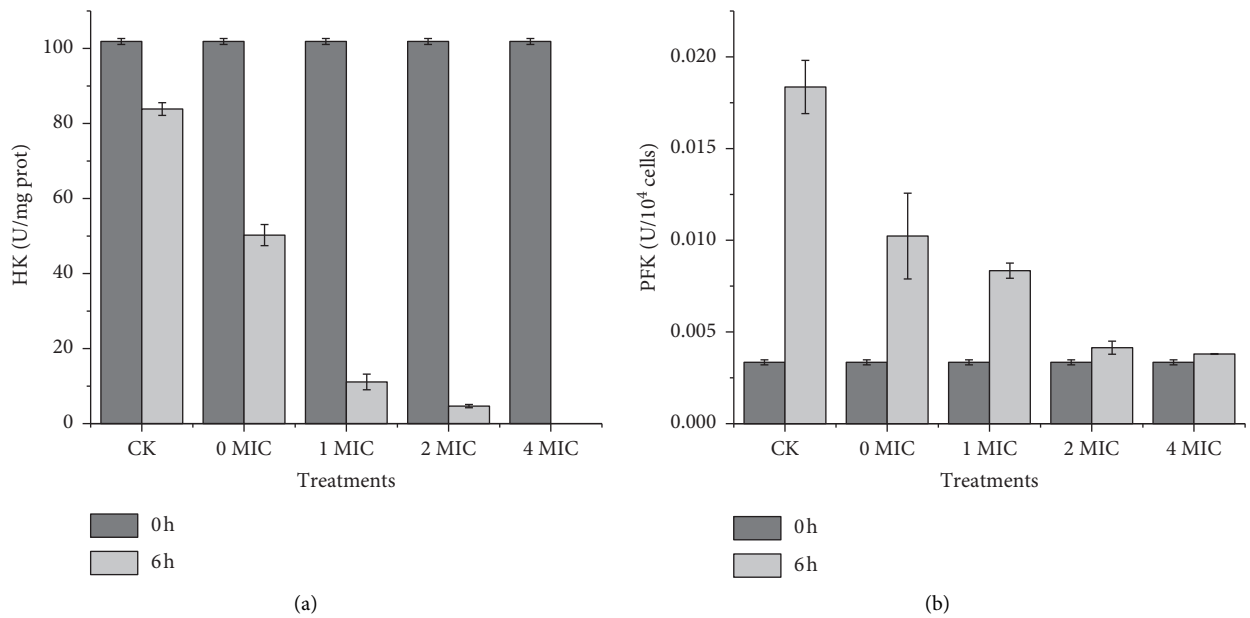


FIGURE 6: Continued.

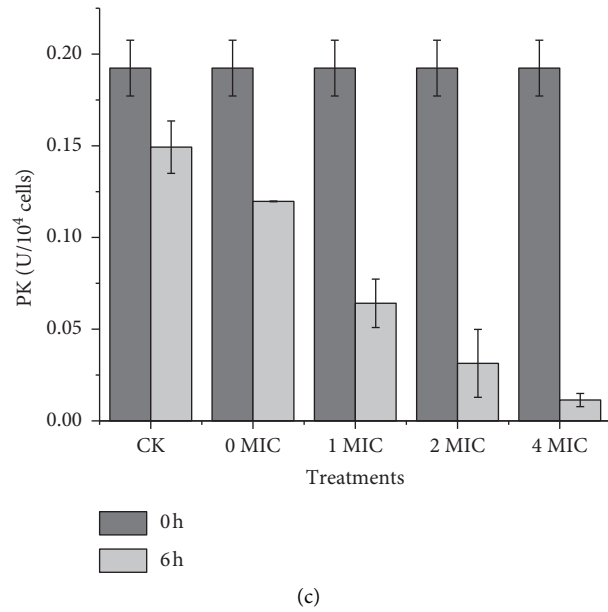


FIGURE 6: Effect of different concentrations of DMY in the EMP pathway on hexokinase (a), phosphofructokinase (b), and pyruvate kinase (c) in *Pseudomonas antarctica*.

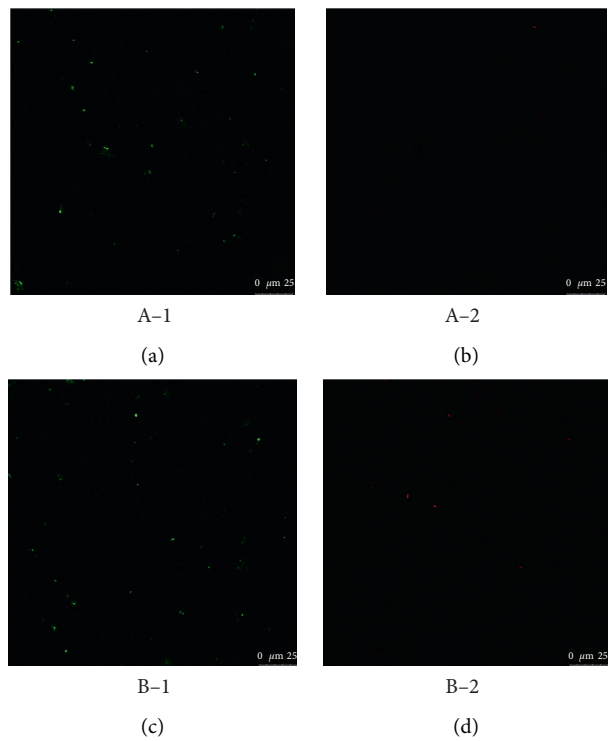


FIGURE 7: Continued.

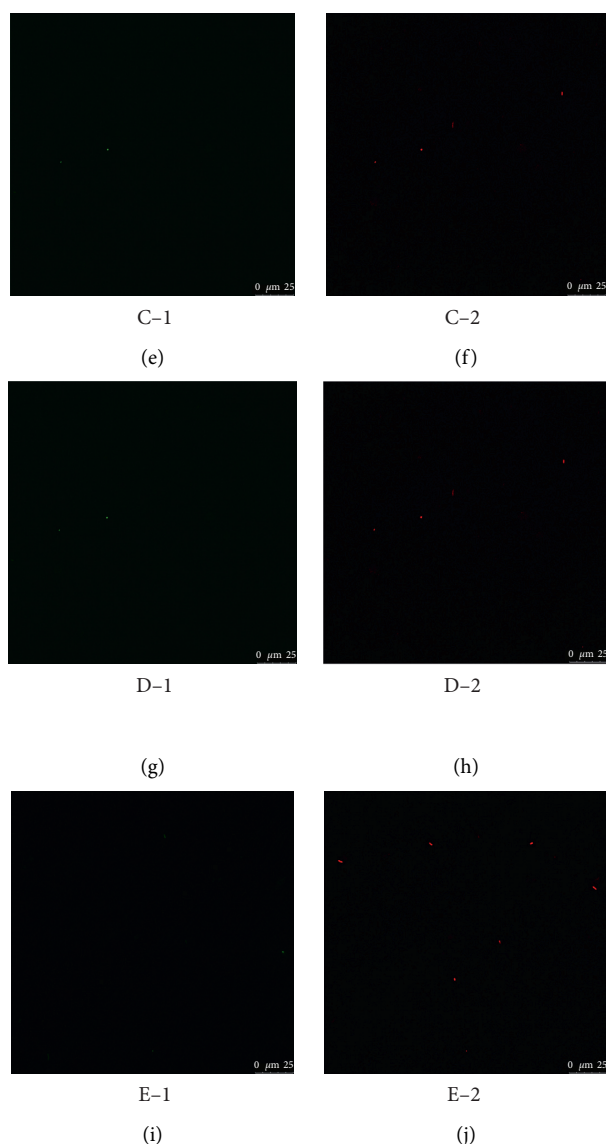


FIGURE 7: Confocal laser scanning microscope (CLSM) of *P. antarctica* at 1000 magnification. (a–e) CLSM images stained with AO, which are images of control, treatment by DMY at 0 MIC, 1 MIC, 2 MIC, and 4 MIC. (f–j) CLSM images stained with PI, which are images of control, treatment by DMY at 0 MIC, 1 MIC, 2 MIC, and 4 MIC. Nuclei of living cells show green fluorescence. Nucleic acids in apoptotic cells show red fluorescence.

4. Conclusions

The *P. antarctica* was the dominant spoilage bacterium in grouper. The emulsion is prepared by mixing with chitosan and sodium alginate to solve the problem that DMY is insoluble in water. CLSM images visually confirmed the inhibition effect of DMY against *P. antarctica*. Besides, DMY disrupted the biofilm structure of *P. antarctica* as evidenced by protein and nucleic acid leakage, AKPase leakage, and reduced ATPase activity. DMY also affected the respiratory metabolic pathway of *P. aeruginosa* by inhibiting key enzymes and thereby decreased the metabolic activity and viability of the bacteria. This work proved that DMY had potential as an effective and natural antibacterial in marine products.

Data Availability

The data used to support the findings of this study are available from the corresponding author upon request.

Conflicts of Interest

The authors declare that there are no conflicts of interest regarding the publication of this paper.

Acknowledgments

This research was funded by the National Natural Science Foundation of China (No. 31972142), supported by the China Agriculture Research System (CARS-47), and

Shanghai Municipal Science and Technology Project to Enhance the Capabilities of the Platform (19DZ2284000). The authors thank the Shanghai Science and Technology Commission Public Service Platform Construction Project (No. 17DZ2293400) for providing funding support for this study.

References

- [1] C. A. Campos, M. P. Castro, S. P. Aubourg, and J. B. Velázquez, "Use of natural preservatives in seafood," in *Novel Technologies in Food Science: Their Impact on Products, Consumer Trends and the Environment*, A. Mcelhatton and P. J. Do Amaral Sobral, Eds., Springer, Berlin, Germany, pp. 325–360, 2012.
- [2] X. Wang, M. Wang, B. Zhou, Y. Zhao, D. Fan, and K. Cheng, "Unraveling the inhibitory effect of dihydromyricetin on heterocyclic aromatic amines formation," *Journal of the Science of Food & Agriculture*, vol. 98, no. 5, pp. 1988–1994, 2018.
- [3] B. Alipour, B. Rashidkhani, and S. Edalati, "Dietary flavonoid intake, total antioxidant capacity and lipid oxidative damage: a cross-sectional study of Iranian women," *Nutrition*, vol. 32, no. 5, pp. 566–572, 2016.
- [4] B. Liu, W. Li, T. A. Nguyen, and J. Zhao, "Empirical, thermodynamic and quantum-chemical investigations of inclusion complexation between flavanones and (2-hydroxypropyl)-cyclodextrins," *Food Chemistry*, vol. 134, no. 2, pp. 926–932, 2012.
- [5] C. Wang, W. Xiong, S. Reddy Perumalla, J. Fang, and C. Calvin Sun, "Solid-state characterization of optically pure (+) Dihydromyricetin extracted from *Ampelopsis grosedentata* leaves," *International Journal of Pharmaceutics*, vol. 511, no. 1, pp. 245–252, 2016.
- [6] X. L. Hou, Q. Tong, W. Q. Wang et al., "Suppression of inflammatory responses by dihydromyricetin, a flavonoid from *ampelopsis grosedentata*, via inhibiting the activation of NF- κ B and MAPK signaling pathways," *Journal of Natural Products*, vol. 78, no. 7, pp. 1689–1696, 2015.
- [7] T. T. Liu, Y. Zeng, K. Tang, X. Chen, W. Zhang, and X. L. Xu, "Dihydromyricetin ameliorates atherosclerosis in LDL receptor deficient mice," *Atherosclerosis*, vol. 262, pp. 39–50, 2017.
- [8] W. Liao, Z. Ning, L. Ma et al., "Recrystallization of dihydromyricetin from *ampelopsis grosedentata* and its antioxidant activity evaluation," *Rejuvenation Research*, vol. 17, no. 5, pp. 422–429, 2014.
- [9] Y. Wu, J. Bai, K. Zhong, Y. Huang, and H. Gao, "A dual antibacterial mechanism involved in membrane disruption and DNA binding of 2 R, 3 R-dihydromyricetin from pine needles of *Cedrus deodara* against *Staphylococcus aureus*," *Food Chemistry*, vol. 218, pp. 463–470, 2017.
- [10] A. Maillat, A. Bouju-Albert, S. Roblin et al., "Impact of DNA extraction and sampling methods on bacterial communities monitored by 16S rDNA metabarcoding in cold-smoked salmon and processing plant surfaces," *Food Microbiology*, vol. 95, Article ID 103705, 2021.
- [11] J. Park and E. B. Kim, "Insights into the gut and skin microbiome of freshwater fish, smelt (*Hypomesus nipponensis*)," *Current microbiology*, vol. 78, pp. 1798–1806, 2021.
- [12] S. Skirnisdóttir, S. Knobloch, H. L. Lauzon et al., "Impact of onboard chitosan treatment of whole cod (*Gadus morhua*) on the shelf life and spoilage bacteria of loins stored superchilled under different atmospheres," *Food Microbiology*, vol. 97, Article ID 103723, 2021.
- [13] W. Huang and J. Xie, "Characterization of the volatiles and quality of hybrid grouper and their relationship to changes of microbial community during storage at 4 degrees C," *Molecules*, vol. 25, no. 4, 2020.
- [14] M. A. M. Hussein, M. Grinholc, A. S. A. Dena, I. M. El-Sherbiny, and M. Megahed, "Boosting the antibacterial activity of chitosan-gold nanoparticles against antibiotic-resistant bacteria by *Punicagranatum* L. extract," *Carbohydrate Polymers*, vol. 256, Article ID 117498, 2021.
- [15] W. Hu, C. Li, J. Dai, H. Cui, and L. Lin, "Antibacterial activity and mechanism of *Litsea cubeba* essential oil against methicillin-resistant *Staphylococcus aureus* (MRSA)," *Industrial Crops and Products*, vol. 130, pp. 34–41, 2019.
- [16] S. Woranuch and R. Yoksan, "Eugenol-loaded chitosan nanoparticles: I. thermal stability improvement of eugenol through encapsulation," *Carbohydrate Polymers*, vol. 96, no. 2, pp. 578–585, 2013.
- [17] F. Yang, S. Jia, J. Liu et al., "The relationship between degradation of myofibrillar structural proteins and texture of superchilled grass carp (*Ctenopharyngodon idella*) fillet," *Food Chemistry*, vol. 301, Article ID 125278, 2019.
- [18] S. Phunpee, S. Saesoo, I. Sramala et al., "A comparison of eugenol and menthol on encapsulation characteristics with water-soluble quaternized β -cyclodextrin grafted chitosan," *International Journal of Biological Macromolecules*, vol. 84, pp. 472–480, 2016.
- [19] R. Cai, M. Zhang, L. Cui et al., "Antibacterial activity and mechanism of thymol against *Alicyclobacillus acidoterrestris* vegetative cells and spores," *LWT (Lebensmittel-Wissenschaft & Technologie)*, vol. 105, pp. 377–384, 2019.
- [20] L. Lin, Y. Gu, C. Li, S. Vittayapadung, and H. Cui, "Antibacterial mechanism of ϵ -poly-L-lysine against *Listeria monocytogenes* and its application on cheese," *Food Control*, vol. 91, pp. 76–84, 2018.
- [21] N. Zhang, W. Lan, Q. Wang, X. Sun, and J. Xie, "Antibacterial mechanism of Ginkgo biloba leaf extract when applied to *Shewanella putrefaciens* and Saprophytic staphylococcus," *Aquaculture and Fisheries*, vol. 3, no. 4, pp. 163–169, 2018.
- [22] K. Li, G. Guan, J. Zhu, H. Wu, and Q. Sun, "Antibacterial activity and mechanism of a laccase-catalyzed chitosan-gallic acid derivative against *Escherichia coli* and *Staphylococcus aureus*," *Food Control*, vol. 96, pp. 234–243, 2019.
- [23] A. J. F. Dalcin, C. G. Santos, S. S. Gündel et al., "Anti biofilm effect of dihydromyricetin-loaded nanocapsules on urinary catheter infected by *Pseudomonas aeruginosa*," *Colloids and Surfaces B: Biointerfaces*, vol. 156, pp. 282–291, 2017.
- [24] Q. Zhang, Y. Zhao, M. Zhang, Y. Zhang, H. Ji, and L. Shen, "Recent advances of vine tea, a potential and functional herbal tea with dihydromyricetin and myricetin as major bioactive compounds," *Journal of Pharmaceutical Analysis*, 2020, In press.
- [25] M.-J. Choi, A. Soottitantawat, O. Nuchuchua, S.-G. Min, and U. Ruktanonchai, "Physical and light oxidative properties of eugenol encapsulated by molecular inclusion and emulsion-diffusion method," *Food Research International*, vol. 42, no. 1, pp. 148–156, 2009.
- [26] O. Nuchuchua, S. Saesoo, I. Sramala, S. Puttipipatkachorn, A. Soottitantawat, and U. Ruktanonchai, "Physicochemical investigation and molecular modeling of cyclodextrin complexation mechanism with eugenol," *Food Research International*, vol. 42, no. 8, pp. 1178–1185, 2009.
- [27] Y. Zhang, J. Wei, Y. Yuan, and T. Yue, "Diversity and characterization of spoilage-associated psychrotrophs in food

- in cold chain,” *International Journal of Food Microbiology*, vol. 290, pp. 86–95, 2019.
- [28] M. K. Remanan and F. Zhu, “Encapsulation of rutin using quinoa and maize starch nanoparticles,” *Food Chemistry*, vol. 353, Article ID 128534, 2020.
- [29] R. Radwan, A. Abdelkader, H. A. Fathi, M. Elsabahy, G. Fetih, and M. El-Badry, “Development and evaluation of letrozole-loaded hyaluronic acid/chitosan-coated poly(D,L-lactide-co-glycolide) nanoparticles,” *Journal of Pharmaceutical Innovation*, vol. 12, 2021.
- [30] D. R. Telange, S. P. Jain, A. M. Pethe, P. S. Kharkar, and N. R. Rarokar, “Use of combined nanocarrier system based on chitosan nanoparticles and phospholipids complex for improved delivery of ferulic acid,” *International Journal of Biological Macromolecules*, vol. 171, pp. 288–307, 2021.
- [31] R. Di Pasqua, G. Betts, N. Hoskins, M. Edwards, D. Ercolini, and G. Mauriello, “Membrane toxicity of antimicrobial compounds from essential oils,” *Journal of Agricultural and Food Chemistry*, vol. 55, no. 12, pp. 4863–4870, 2007.
- [32] P.-Y. Xu, C.-P. Fu, R. K. Kankala, S.-B. Wang, and A.-Z. Chen, “Supercritical carbon dioxide-assisted nanonization of dihydromyricetin for anticancer and bacterial biofilm inhibition efficacies,” *The Journal of Supercritical Fluids*, vol. 161, Article ID 104840, 2020.
- [33] H. Cui, C. Zhang, C. Li, and L. Lin, “Antimicrobial mechanism of clove oil on *Listeria monocytogenes*,” *Food Control*, vol. 94, pp. 140–146, 2018.
- [34] G. Liguri, N. Taddei, P. Nassi, S. Latorraca, C. Nediani, and S. Sorbi, “Changes in Na^+ , K^+ -ATPase, Ca^{2+} -ATPase and some soluble enzymes related to energy metabolism in brains of patients with Alzheimer’s disease,” *Neuroscience Letters*, vol. 112, no. 2, pp. 338–342, 1990.
- [35] S. N. Khan, S. Khan, J. Iqbal, R. Khan, and A. U. Khan, “Enhanced killing and antibiofilm activity of encapsulated cinnamaldehyde against *Candida albicans*,” *Frontiers in Microbiology*, vol. 8, p. 1641, 2017.
- [36] Á. Luís, F. Silva, S. Sousa, A. P. Duarte, and F. Domingues, “Antistaphylococcal and biofilm inhibitory activities of gallic, caffeic, and chlorogenic acids,” *Biofouling*, vol. 30, no. 1, pp. 69–79, 2014.
- [37] J. Zhu, X. Huang, F. Zhang, L. Feng, and J. Li, “Inhibition of quorum sensing, biofilm, and spoilage potential in *Shewanella baltica* by green tea polyphenols,” *Journal of Microbiology*, vol. 53, no. 12, pp. 829–836, 2015.
- [38] J.-R. Bai, K. Zhong, Y.-P. Wu, G. Elena, and H. Gao, “Antibiofilm activity of shikimic acid against *Staphylococcus aureus*,” *Food Control*, vol. 95, pp. 327–333, 2019.